

## **AuPS/ASB Meeting - Newcastle 2007**

### **Free communications: Cardiac muscle**

Wednesday 5 December 2007 – Mulubinba Room

Chair: David Allen

## Hyperinsulinaemia and elevated levels of phosphorylated Akt/PKB in the neonatal Hypertrophic Heart Rat (HHR) precede the onset of cardiac hypertrophy

E.R. Porrello,<sup>1,2</sup> J.D. Schertzer,<sup>1</sup> C.L. Curl,<sup>1</sup> W.F. Meeker,<sup>1</sup> K.M. Mellor,<sup>1</sup> G.S. Lynch,<sup>1</sup> S.B. Harrap,<sup>1</sup> W.G. Thomas<sup>2</sup> and L.M.D. Delbridge,<sup>1</sup> <sup>1</sup>Department of Physiology, The University of Melbourne, Parkville, VIC 3010, Australia and <sup>2</sup>Baker Heart Research Institute, Prahran, VIC 3004, Australia.

There is experimental and epidemiological evidence supporting the 'foetal origins of adult disease' hypothesis. It is well established that low birth weight is associated with increased cardiovascular risk and diabetes in adulthood. However, relatively little is known about the molecular and cellular mechanisms controlling neonatal programming of adult cardiovascular disease. Cardiac hypertrophy is a major cardiovascular risk factor and is often seen in association with diabetes. The developmental origins of this condition have not been extensively studied. The Hypertrophic Heart Rat (HHR) is a normotensive model of cardiac and cardiomyocyte hypertrophy (Harrap *et al.*, 2002). The aim of this study was to determine whether the growth-regulating protein kinase PKB/Akt is implicated in the neonatal 'programming' of the HHR adult cardiac phenotype.

HHR and control strain Normal Heart Rat (NHR) neonates were killed by decapitation at post-natal day 2. Male NHR and HHR were also culled at 4, 6, 8 and 12 weeks of age ( $n = 8-11$  per group) by overdose of halothane. Hearts were immediately excised post-mortem and cardiac mass was normalized to body mass to give a cardiac weight index (CWI, mg/g). Trunk blood was collected from fasted (30 min for neonates and overnight for 12 week old) NHR and HHR for analysis of blood glucose (glucometer, Accu-Check<sup>®</sup>) and plasma insulin (radioimmunoassay, Linco Research) levels. At post-natal day 2, HHR hearts were significantly smaller than NHR ( $4.33 \pm 0.19$  vs.  $5.01 \pm 0.08$  mg/g,  $p = 0.024$ ). HHR hearts were similar to NHR by 4 weeks ( $5.10 \pm 0.15$  vs.  $5.16 \pm 0.11$  mg/g) and were 11% larger than NHR by 8 weeks of age. This was followed by a rapid period of growth, and by 12 weeks of age HHR CWIs were 27% larger than NHR ( $p = 0.003$ ). Blood glucose and plasma insulin levels were both significantly higher in HHR neonates (glucose:  $3.51 \pm 0.16$  vs.  $5.00 \pm 0.12$  mM; insulin:  $0.68 \pm 0.06$  vs.  $2.07 \pm 0.27$  ng/ml,  $p < 0.001$ ). At 12 weeks of age, HHR were still hyperglycaemic ( $5.97 \pm 0.35$  vs.  $8.08 \pm 0.43$  mM,  $p < 0.01$ ), but plasma insulin levels were not different ( $2.69 \pm 0.91$  vs.  $2.34 \pm 0.62$  ng/ml).

Phosphorylated (Ser473) and total Akt levels were determined in NHR and HHR neonatal and 12 week old ventricular lysates by western blot. The ratio of phosphorylated to total Akt was 2.3-fold higher in the HHR heart at post-natal day 2 ( $0.99 \pm 0.07$  vs.  $2.31 \pm 0.53$ ,  $p = 0.029$ ), but was not significantly different at 12 weeks of age ( $1.00 \pm 0.05$  vs.  $1.14 \pm 0.09$ ,  $p = 0.18$ ). As Akt suppresses cardiomyocyte apoptosis, we sought to quantify the incidence of apoptosis in the HHR neonatal heart. Cryosections from the mid-ventricle of post-natal day 2 rats were stained with TUNEL to label apoptotic nuclei. Sections were counter-stained with DAPI to label total nuclei. The number of TUNEL positive cells in the myocardium was normalized to the total area of DAPI stained nuclei to obtain an apoptotic index. The apoptotic index was suppressed almost 3-fold in the neonatal HHR heart ( $0.002 \pm 0.0005\%$  vs.  $0.0007 \pm 0.0002\%$ ,  $p = 0.02$ ).

These findings demonstrate that cardiac growth restriction and hyperinsulinaemia in the neonate precede the onset of cardiac hypertrophy in the HHR. The hyperactivation of Akt signalling and suppression of myocardial apoptosis in the neonatal HHR heart may implicate these molecular and cellular mechanisms in the neonatal 'programming' of adult cardiovascular disease.

Harrap SB, Danes VR, Ellis JA, Griffiths CD, Jones EF & Delbridge LM. (2002) *Physiological Genomics*, **9**: 43-8.

## Regulation of ryanodine receptors from cardiac muscle by luminal Ca<sup>2+</sup> and Mg<sup>2+</sup>

D.R. Laver, School of Biomedical Sciences, University of Newcastle and Hunter Medical Research Institute, Callaghan, NSW 2308, Australia.

Muscle contraction occurs when Ca<sup>2+</sup> is released from the sarcoplasmic reticulum (SR) through ryanodine receptor Ca<sup>2+</sup> release channels (RyRs). In heart, uptake and release of Ca<sup>2+</sup> from the SR causes the free [Ca<sup>2+</sup>]<sub>L</sub> within the lumen ([Ca<sup>2+</sup>]<sub>L</sub>) to cycle between ~0.3 to 1.0 mmol/l during the normal heart beat (Ginsburg *et al.*, 1998). [Ca<sup>2+</sup>]<sub>L</sub> is known to regulate the Ca<sup>2+</sup> releasing excitability of this store by stimulating the RyRs in its membrane. The resulting negative feedback between store depletion and Ca<sup>2+</sup> release is believed to drive pacemaking and rhythmicity cardiac muscle (Vinogradova *et al.*, 2005) as well as smooth muscle (Van Helden, 1993) and neurons (Verkhatsky, 2005). Luminal stimulation of RyRs involves three Ca<sup>2+</sup> sensing mechanisms on both the luminal and cytoplasmic side of the RyR (Laver, 2007); namely the luminal Ca<sup>2+</sup>-activation site (*L*-site, 60 μmol/l affinity), the cytoplasmic activation site (*A*-site, 0.9 μmol/l affinity) and the high affinity cytoplasmic Ca<sup>2+</sup>-inactivation site (*I*<sub>2</sub>-site, 1.2 μmol/l affinity). Cardiac RyR (RyR2 isoform) activation by luminal Ca<sup>2+</sup> occurs by a multi-step process dubbed "luminal-triggered Ca<sup>2+</sup> feed-through". Ca<sup>2+</sup> binding to the *L*-site initiates channel openings where upon luminal Ca<sup>2+</sup> can flow through to the *A*-site (producing prolongation of openings) and to the *I*<sub>2</sub>-site (causing inactivation at high levels of Ca<sup>2+</sup> feed-through). Cytoplasmic Mg<sup>2+</sup> inhibits RyRs by displacing Ca<sup>2+</sup> from the *A*-site (Laver *et al.*, 1997) and plays an important role in regulating Ca<sup>2+</sup> release. However, the possibility that similar processes occur at the *L*- and *I*<sub>2</sub>-sites has not been explored.

To explore this possibility, single RyRs and RyR arrays were incorporated into artificial lipid bilayers. SR vesicles were prepared from sheep hearts. Animals were killed by barbiturate overdose prior to muscle removal. SR vesicles containing RyRs were incorporated into artificial planar lipid bilayers which separated baths corresponding to the cytoplasm and SR lumen. The baths contained 230 mmol/l CsCH<sub>3</sub>O<sub>3</sub>S, 20 mmol/l CsCl, 10 mmol/l TES (pH 7.4) plus various amounts of Ca<sup>2+</sup>, Mg<sup>2+</sup> and ATP. Channel activity was recorded using Cs<sup>+</sup> as the current carrier. A novel, high affinity inhibition of RyR2 by luminal Mg<sup>2+</sup> was observed, pointing to an important physiological role for luminal Mg<sup>2+</sup> in cardiac muscle. At diastolic cytoplasmic [Ca<sup>2+</sup>]<sub>C</sub> ([Ca<sup>2+</sup>]<sub>C</sub> = 100 nmol/l) luminal Mg<sup>2+</sup> inhibition was voltage-independent and was alleviated by increasing luminal [Ca<sup>2+</sup>]<sub>L</sub>. The *K*<sub>i</sub> for Mg<sup>2+</sup> inhibition increased from 90 μmol/l at [Ca<sup>2+</sup>]<sub>L</sub> = 0.3 mmol/l to 1 mmol/l at [Ca<sup>2+</sup>]<sub>L</sub> = 1 mmol/l. At systolic [Ca<sup>2+</sup>]<sub>C</sub> (1- 10 μmol/l), Mg<sup>2+</sup> inhibition was substantially reduced and its properties were consistent with luminal Mg<sup>2+</sup> flowing through the channel and binding to the cytoplasmic *A*-site. Under these conditions *K*<sub>i</sub> was voltage-dependent; 13 mmol/l at -40 mV and >100 mmol/l at +40 mV. The data could be accurately fitted by a model in which Mg<sup>2+</sup> and Ca<sup>2+</sup> compete at both the *L*- and *A*-sites and where the *L*-site has similar affinities for both ions. The model predicts that under physiological divalent ion concentrations (1 mmol/l free Mg<sup>2+</sup> in the cytoplasm and lumen) and membrane potential (0 mV), [Ca<sup>2+</sup>]<sub>L</sub> activation of Ca<sup>2+</sup> release is primarily due to displacement of Mg<sup>2+</sup> from the *L*-site and that luminal Mg<sup>2+</sup> is an essential cofactor for the phenomenon. Therefore competition between luminal Ca<sup>2+</sup> and Mg<sup>2+</sup> may play an essential role in store-load dependent Ca<sup>2+</sup> release.

Ginsburg KS, Weber CR & Bers DM. (1998) *Journal General Physiology*, **111**: 491-504.

Vinogradova TM, Maltsev VA, Bogdanov KY, Lyashkov AE & Lakatta EG. (2005) *Annals of the New York Academy of Sciences*, **1047**: 138-156

Van Helden DFJ. (1993) *Journal of Physiology*, **471**: 465-79.

Verkhatsky A. (2005) *Physiological Reviews*, **85**: 201-79.

Laver DR. (2007) *Biophysical Journal*, **92**: 3541-55.

Laver DR, Baynes TM & Dulhunty AF. *Journal of Membrane Biology*, **156**: 213-29.

## ***In vitro* modulation of the cardiac ryanodine receptor (calcium release channel) activity by human homer 1b**

P. Pouliquin, S.M. Pace and A.F. Dulhunty, Division of Molecular Bioscience, John Curtin School of Medical Research, Australian National University, Canberra ACT 0200, Australia.

Calcium signalling controls a wide variety of physiological processes and depends on the activity of protein signalling complexes which are clustered in specialised cellular sites. Ryanodine receptor (RyR) calcium release channels form the hub of the calcium signalling complex that is vital in muscle contraction. The Homer protein family allows both clustering and functional modulation of a plethora of different calcium signalling complexes. Homer 1 has recently been implicated in the interaction between RyR2 and a surface membrane L-type  $\text{Ca}^{2+}$  channel (dihydropyridine receptor, or  $\text{Ca}_v1.2$ ) in the mice urinary bladder (Huang *et al.*, 2007). *In vitro* studies indicate that Homer 1b/c activates the skeletal muscle RyR1 (Pouliquin *et al.*, 2006 and Feng *et al.*, 2007) while it inhibits RyR2, the main RyR isoform in the heart and in neurons (Westhoff *et al.*, 2003). In the present study, we revisit the *in vitro* regulation of RyR2 by Homer 1.

New Zealand male white rabbits were euthanized by a captive bolt and back and leg muscle used to prepare skeletal sarcoplasmic vesicles. Cardiac sarcoplasmic vesicles were isolated from Merino sheep euthanized by overdose of 20 ml valbarb euthanasia solution (300 mg/ml) injected into the jugular vein. All sarcoplasmic vesicles were stored in liquid nitrogen. Human Homer 1b (H1b) fusion protein (with C-myc and 6His tags) was expressed in *E. Coli* and affinity purified on Ni-agarose columns (Pouliquin *et al.*, 2006). Sequence encoding human Homer 1b 120 N-term residues (Short Homer) was amplified by PCR and subcloned into the plasmid pHUE, Short Homer fusion protein was expressed and purified in the same way as H1b. Purified fusion proteins were dialysed overnight at 4°C against >1000 volumes of PBS, aliquots were stored at -80°C. Protein purity and identity were assessed using SDS-PAGE and Western blotting after electro-transfer onto nitrocellulose. Primary and secondary antibodies were monoclonal anti-C-myc and anti-mouse IgG POD conjugated (Sigma), immuno-decorated proteins were revealed by chemiluminescence (Roche). Activity of RyR present in sarcoplasmic vesicles was assessed from [ $^3\text{H}$ ] ryanodine binding (which increases when channel open probability increases) and from RyR channels incorporated into artificial lipid bilayers.

We show here that the *in vitro* activity of RyR2 is modulated in a complex manner by human Homer1b. Both ryanodine binding and single channel recordings indicated that at resting and activating cytosolic calcium concentrations, Homer1b, and a shorter version of the protein lacking the coil-coil domain, activated RyR2 in a dose dependent manner, in contrast to previously reported actions of Homer 1 (Westhoff *et al.*, 2003). Maximum activity was reached with ~500 nM Homer1, and activity fell with higher Homer concentration. Homer1b increased RyR2 activity at all cytosolic  $\text{Ca}^{2+}$  concentrations without altering the  $\text{Ca}^{2+}$  concentration dependence of RyR2 activity (RyR2 was active in the same  $\text{Ca}^{2+}$  concentration range and reached its maximal activity at the same  $\text{Ca}^{2+}$  concentration either in the absence or in the presence of Homer1 b). When RyR2 was maximally activated by 100  $\mu\text{M}$  cytosolic calcium, RyR2 modulation by Homer1 b was complex: RyR2 activity was inhibited by ~10 nM Homer1 b and >500 nM Homer1 b, while intermediate concentrations activated the channel. These results show conclusively that Homer would activate  $\text{Ca}^{2+}$  release in the heart, as in skeletal muscle, in the presence of physiological cytoplasmic  $\text{Ca}^{2+}$  concentrations. We suggest that the differences between the results obtained in the present study and previously reported data (Westhoff *et al.*, 2003) may be due to different intrinsic properties of RyR2 from different species. Rodent Homer1 c was shown to inhibit rodent RyR2 activity in various conditions (Westhoff *et al.*, 2003), while we show that human Homer1 b modulates sheep RyR2. These two Homer1 proteins are highly homologous and to date no functional difference between them has been reported, while clear differences in the regulation of RyR2 from different species by other crucial proteins has been reported (Jeyakumar *et al.*, 2001). The complex modulation of RyR2 by Homer1 b is physiologically relevant in the heart and in neurons, where high levels of the two proteins are expressed.

Huang G, Kim JY, Dehoff M, Mizuno Y, Kamm KE, Worley PF, Muallem S & Zeng W. (2007) *Journal of Biological Chemistry*, **282**: 14283-90.

Pouliquin P, Pace SM, Curtis SM, Harvey PJ, Gallant EM, Zorzato F, Casarotto MG & Dulhunty AF. (2006) *International Journal of Biochemistry and Cell Biology*, **38**: 1700-15.

Feng W, Tu J, Pouliquin P, Cabrales E, Shen X, Dulhunty A, Worley PF, Allen PD and Pessah IN. (2007) *Cell Calcium*, in press

Westhoff JH, Hwang SY, Duncan RS, Ozawa F, Volpe P, Inokuchi K & Koulen P. (2003) *Cell Calcium*, **34**: 261-9.

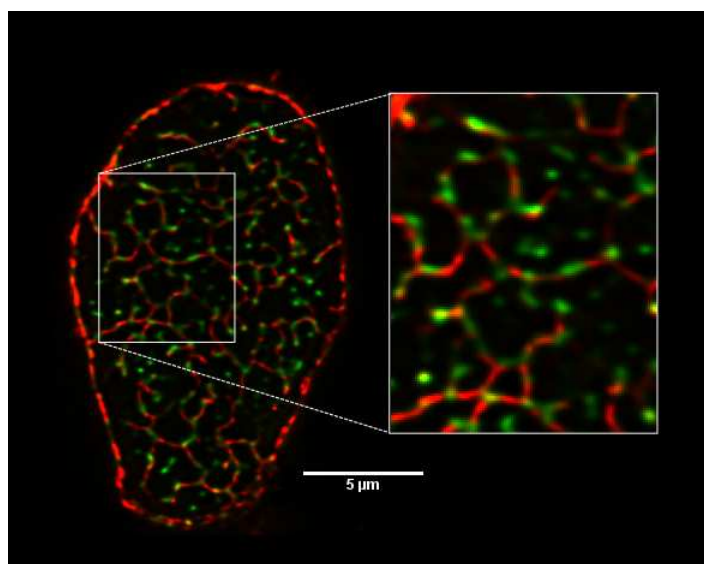
Jeyakumar LH, Ballester L, Cheng DS, McIntyre JO, Chang P, Olivey HE, Rollins-Smith L, Barnett JV, Murray K, Xin HB & Fleischer S. (2001) *Biochemical and Biophysical Research Communications*, **281**: 979-86.

## Visualization of the 3-D distribution of proteins involved in cardiac excitation-contraction coupling using a novel optical approach

I.D. Jayasinghe, M.B. Cannell and C. Soeller, Department of Physiology, Faculty of Medical and Health Sciences, 85 Park Road, Grafton, Auckland, New Zealand.

Ca<sup>2+</sup> induced release of Ca<sup>2+</sup> from the sarcoplasmic reticulum (SR) triggered by voltage-dependent transsarcolemmal Ca<sup>2+</sup> fluxes is thought to form the basis of excitation-contraction (EC) coupling in cardiac myocytes. Close apposition of the sarcolemmal membrane with the SR Ca<sup>2+</sup> release channels or ryanodine receptors (RyRs) is essential to achieving the rapid Ca<sup>2+</sup> release that ensures cardiac contraction. The sarcolemmal membrane architecture is complex, with the presence of caveolar invaginations and a dense network of t-tubules near each z-disk. Such complexity in the organization of membrane structures and the compact arrays of key proteins central to EC coupling is only partially resolved when imaged by confocal microscopy. The resolution can be effectively improved by using a recently-demonstrated technique (Chen-Izu *et al.*, 2006) to image these fine elements of the sarcolemma in single cells oriented vertically on the microscope stage. We have used this approach to visualize the distribution of the Na-Ca exchanger (NCX), Caveolin-3 (Cav3, a marker for caveolar membrane invaginations) and RyRs in enzymatically isolated and fixed rat myocytes at high resolution. The distribution of Caveolin-3 (red) and RyR (green) labelling in a single z-disk of a rat ventricular myocyte is shown in the figure below illustrating the level of detail that is achieved.

Combined with digital 3-D deconvolution to further improve contrast and signal-to-noise ratio, we employed this novel method to resolve the distribution of NCX relative to the sites of SR Ca<sup>2+</sup> release that are apparent as clusters of RyR labelling (Soeller & Cannell, 2007). It has been suggested that reverse mode exchange via NCX may contribute towards triggering SR Ca<sup>2+</sup> release in rat myocytes (Bridge *et al.*, 2003, Lines *et al.*, 2006), but the putative junctional localisation of NCX implied by these studies has been somewhat unclear due to the lack of techniques with sufficient spatial resolution. While NCX labelling generally followed the geometry of the t-system (as outlined by Cav3 labelling), more intense labelling of the exchanger was observed at regularly-spaced domains along z-line-associated t-tubules. Analysis of double-labelled cells indicated that some but not all RyR clusters colocalize with NCX labelling and at least 10% of the total NCX labelling was located at or near junctions.



While NCX labelling generally followed the geometry of the t-system (as outlined by Cav3 labelling), more intense labelling of the exchanger was observed at regularly-spaced domains along z-line-associated t-tubules. Analysis of double-labelled cells indicated that some but not all RyR clusters colocalize with NCX labelling and at least 10% of the total NCX labelling was located at or near junctions.

Recently, it has been suggested that some RyR clusters found distal to z-lines are not associated with junctions (Lukyanenko *et al.*, 2007). Our data show that RyR clusters located between z-lines are generally closely associated with longitudinal elements of the t-system (Soeller & Cannell, 1999) as identified by NCX and Cav3 labelling. Thus these RyR clusters are likely in junctions with the longitudinal t-system.

Our data provide 3D data sets for detailed modelling studies to improve our understanding of the potential role of NCX in modulating SR release.

Bridge JHB, Inoue M & Cannell MB. (2003) *Journal of Molecular and Cellular Cardiology*, **35**: A14.

Chen-Izu Y, McCulle S, Ward CW, Soeller C, Allen BG, Rabang C, Cannell MB, Balke CW & Izu LT. (2006) *Biophysical Journal*, **91**: 1-13.

Lines GT, Sande JB, Louch WE, Mork HK, Grottm P & Sejersted OM. (2006) *Biophysical Journal*, **91**: 779-92.

Lukyanenko V, Ziman A, Lukyanenko A, Salnikov V & Lederer WJ. (2007) *Journal of Physiology*, **583**: 251-269.

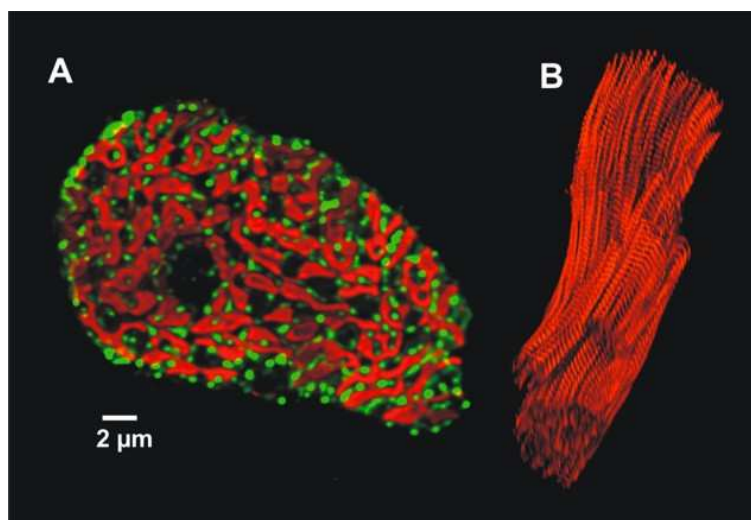
Soeller C & Cannell MB. (1999) *Circulation Research*, **84**: 266-75.

Soeller C, Crossman D, Gilbert R & Cannell MB. (2007) *Proceedings of the National Academy of Science of the United States of America*, **104**: 14958-63.

## Analysis of ryanodine receptor clusters in rat and human cardiac myocytes at high optical resolution

C. Soeller, R. Gilbert, D. Crossman and M.B. Cannell, Department of Physiology, School of Medical Sciences, University of Auckland, Private Bag 92019, Auckland, New Zealand.

The molecular basis of 'local control' of cardiac excitation-contraction (E-C) coupling resides in the gating of sarcoplasmic reticulum (SR)  $\text{Ca}^{2+}$  release channels or ryanodine receptors (RyRs) which are clustered in the junctions between terminal SR and the transverse tubular system. We have determined the localization of RyR clusters and simultaneously visualized the location of the contractile apparatus by antibody labelling. Using a novel confocal imaging protocol (Chen-Izu *et al.*, 2006) we were able to resolve all the clusters within a z-disk at very high optical resolution ( $\sim 250$  nm) in single rat ventricular myocytes and human ventricle tissue sections. For optimal resolution it was critical to maximize image contrast by refractive index matching and deconvolution. The RyR label formed discrete puncta representing clusters of RyRs or 'couplons' around the edges of the myofilaments (see Figure, panel A) with a nearest neighbour spacing of  $0.66 \pm 0.06 \mu\text{m}$  in rat and  $0.78 \pm 0.07 \mu\text{m}$  in human (Soeller *et al.*, 2007). Each bundle of myofibrils was served by  $\sim 6$  couplons which supplied a cross-sectional area of  $\sim 0.6 \mu\text{m}^2$  in rat and  $\sim 0.8 \mu\text{m}^2$  in human. While the couplons were in reasonable registration with z-lines, the  $\alpha$ -actinin labeling (see Figure, Panel B) revealed discontinuities in the longitudinal position of sarcomeres across the cell so that dislocations in the order of RyR clusters occurred. By quantifying the labelling intensity in rat ventricular myocytes based on antibody binding, a lower limit of 78 RyRs per cluster (on average) was obtained. With a new calibration method that uses optically resolved clusters to calibrate the intensity signal and assuming a geometry where couplons wrap as a disk around a t-tubule, 95% of couplons contained between 120 and 260 RyRs. Our data can explain the spherical propagation of  $\text{Ca}^{2+}$  waves and provide the first quantitative three-dimensional data sets needed for accurate modelling of cardiac CICR and the transition to regenerative release. The 3D information should help improve our understanding of the regulation of cardiac  $\text{Ca}^{2+}$  metabolism.



Chen-Izu Y, McCulle S, Ward C, Soeller C, Allen B, Rabang C, Cannell MB, Balke C & Izu L. (2006) *Biophysical Journal*, **91**: 1-13.

Soeller C, Crossman D, Gilbert R & Cannell MB. (2007) *Proceedings of the National Academy of Sciences USA*, 10.1073/pnas.0703016104.

## Angiotensin II mediates cardiomyocyte growth signalling via ErbB4

H. Chan,<sup>1,2</sup> N.J. Smith,<sup>1</sup> A. Agrotis,<sup>1</sup> R.D. Hannan<sup>3</sup> and W.G. Thomas,<sup>1</sup> <sup>1</sup>Baker Heart Research Institute, Melbourne, VIC 8008, Australia, <sup>2</sup>Department of Biochemistry and Molecular Biology, Monash University, Clayton, VIC 3800, Australia and <sup>3</sup>Peter MacCallum Cancer Centre, East Melbourne, VIC 3002, Australia.

Cardiomyocyte hypertrophy induced by angiotensin II (AngII) is mediated by the type 1 AngII receptor (AT<sub>1</sub>R), a G protein-coupled receptor, which is targeted clinically to alleviate hypertension and the complications of cardiovascular disease. At the cellular level, activated AT<sub>1</sub>Rs promote growth of renal, vascular and cardiac tissues by *transactivating* epidermal growth factor receptors (EGFRs), presumably via shedding of EGF-like ligands and the activation of one or more EGFR family members. Four structurally-conserved EGFR receptor tyrosine kinases exist, and these are termed ErbB1-4. Screening a panel of EGF-like ligands for their capacity to induce cardiomyocyte hypertrophy (measured by changes in protein:DNA ratio of isolated neonatal cardiomyocytes) revealed that betacellulin, neuregulin1- $\beta$ 1 and neuregulin2 $\beta$  (which predominantly act through ErbB4) were the most potent activators ( $147.9 \pm 1.6$ ,  $134.6 \pm 2.0$ , and  $133.7 \pm 2.1\%$  compared to control, respectively). No small molecule selective inhibitors of ErbB4 are available, so we have developed small interfering RNAs that target ErbB4 gene expression (ErbB4 siR) to allow examination of the requirement for ErbB4 in cardiomyocyte hypertrophy. Interestingly, four major splice variants of ErbB4 exist and we used RT-PCR to show that these are all expressed in rat cardiomyocytes as well as whole human heart. Hence, we designed our siR to target a common region of the ErbB4 mRNA sequence and then confirmed efficient knockdown in HEK293 cells transiently expressing the separate ErbB4 isoforms. Using promoter-driven luciferase constructs for genes related to cardiomyocyte growth (ANP, MLC2V and cyclinD), we observed that *pan*knockdown of ErbB4 prevented the ability of neuregulin1/AngII to selectively activate ANP, CycD and MLC2V. This decrease was reversed by co-expression of specific ErbB4 isoforms mutated to make them resistant to siR knockdown, confirming that ErbB4 appears to mediate AngII-dependent cardiomyocyte hypertrophy and that this is mediated in an isoform-specific manner.

## **Hypertrophic cardiomyopathy causing mutations in myosin binding protein-C alter PKA phosphorylation**

C.E. Oakley,<sup>1,2</sup> J. Hwang,<sup>1</sup> L.J. Brown,<sup>3</sup> M. Kekic,<sup>1</sup> P.G. Fajer<sup>2</sup> and B.D. Hambly,<sup>1</sup> <sup>1</sup>Discipline of Pathology, University of Sydney, NSW 2006, Australia, <sup>2</sup>Institute of Molecular Biophysics, Florida State University, Tallahassee, FL 32306, USA and <sup>3</sup>Department of Chemistry and Biomolecular Sciences, Macquarie University, Sydney, NSW 2109, Australia.

Cardiac myosin binding protein C (cMyBPC) is a large regulatory protein within the sarcomere. cMyBPC phosphorylation increases systolic tension, and dissociates the N-terminal region of cMyBPC from the S2 neck region of myosin. cMyBPC mutations are associated with familial hypertrophic cardiomyopathy (FHC). We have cloned, expressed and purified the N-terminal region (immunoglobulin motifs C1 to C2) that encompasses the tri-phosphorylation sites (defined as sites A to C). Using *in vitro* mutagenesis we have also generated four FHC mutant forms of C1-C2. Four FHC-causing mutations are located in the phosphorylatable linker between Ig motifs C1 and C2; G278E, G279A, R326Q and L352P. The effect of these mutations on phosphorylation with PKA at 30°C was investigated. The G279A and R326Q mutations yielded the same rate of phosphorylation as the WT C1-C2; complete di-phosphorylation in less than 5 minutes and complete tri-phosphorylation by 2.5 hours. The G278E mutant was phosphorylated more slowly; complete di-phosphorylation by 30 minutes and complete tri-phosphorylation in > 4 hours. Surprisingly, the L352P construct was phosphorylated more rapidly than WT; complete tri-phosphorylation in 2 hours. In all cases the phosphorylation order was the same as WT (first site B, then A and finally C). Structure prediction provides insights into the mechanisms underlying the changes in phosphorylation rate. Together these data suggest that an alteration in cMyBPC phosphorylation rate may underlie the pathogenesis of FHC caused by some mutations, although paradoxically the rate can be increased or decreased.



## **Novel actin/tropomyosin filaments that regulate glucose uptake and insulin secretion**

A.J. Kee,<sup>1,2</sup> R. Szokolai,<sup>1,3</sup> N. Vlahovich,<sup>1,3</sup> R.G. Parton,<sup>4</sup> D.E. James,<sup>5</sup> G.J. Cooney,<sup>5</sup> P.W. Gunning<sup>2,6</sup> and E.C. Hardeman,<sup>1,2</sup> <sup>1</sup>Muscle Development Unit, Children's Medical Research Institute, Westmead, NSW 2145, Australia, <sup>2</sup>Faculty of Medicine, University of Sydney, NSW 2006, Australia, <sup>3</sup>University of Western Sydney, NSW 1797, Australia, <sup>4</sup>Institute for Molecular Biosciences, University of Queensland, QLD 4072, Australia, <sup>5</sup>Diabetes and Obesity Program, Garvan Institute of Medical Research, NSW 2010, Australia and <sup>6</sup>Oncology Research Unit, Children's Hospital at Westmead, Westmead, NSW 2145, Australia.

Type II Diabetes is Australia's fastest growing chronic disease where its onset is linked to two exocytic processes, altered glucose uptake and insulin secretion. In the former process, the glucose transporter, GLUT4, is trafficked in specialised vesicles to the surface membranes, while insulin secretion occurs through fusion of insulin-containing granules with the pancreatic  $\beta$ -cell surface. The actin cytoskeleton is known to play critical roles in both of these processes. We have identified a novel non-sarcomeric actin filament system in skeletal muscle defined by the tropomyosin (Tm) isoform, Tm5NM1 (Kee *et al.*, 2004). Immunofluorescence microscopy studies on muscle sections and isolated fibres indicate that this filament structure is associated with the T-tubule membrane system, a major site of glucose uptake in muscle. Further immunolocalisation and immunoprecipitation studies indicates that Tm5NM1 interacts with Syntaxin-4, a protein necessary for GLUT4 insertion into the plasma membrane. This suggests a role for Tm5NM1 in GLUT4 trafficking and glucose uptake. To understand the function of this actin/Tm structure we have created tissue-wide Tm5NM1 transgenic (Tg) and knock-out (KO) mice. Insulin tolerance tests revealed that the Tg mice clear glucose from the blood more rapidly than wild-type (WT) mice suggesting that these mice display increased insulin sensitivity ( $p < 0.001$ , *t*-test). Insulin caused a similar increase in Akt phosphorylation, a major upstream regulator of GLUT4 translocation, in skeletal muscle and adipose tissue from both Tg and KO mice suggesting that Tm5NM1 is acting downstream of insulin signalling, consistent with a role in GLUT4 trafficking itself. Glucose tolerance tests revealed that in addition to enhanced insulin sensitivity these animals also displayed ( $p < 0.001$ , *t*-test at all time points), an increase in basal and glucose-stimulated insulin secretion suggesting that Tm5NM1 has a role in pancreatic insulin secretion. In conclusion, we have identified novel actin/Tm filaments that may regulate the exocytic processes of glucose uptake and insulin secretion. The results of these studies have implications for conditions of altered glucose uptake and insulin secretion, such as Type II diabetes and obesity.

Kee AJ, Schevzov G, Nair-Shalliker V, Robinson CS, Vrhovski B, Ghoddusi M, Qiu MR, Lin JJ, Weinberger R, Gunning PW & Hardeman EC. (2004) *Journal of Cell Biology*, **166**: 685-96.